Geophysical Research Letters

RESEARCH LETTER
10.1029/2025GL116648

Key Points:

- The trans-seasonal El Niño-Southern Oscillation-western North Pacific anomalous circulation (ENSO-WNPAC) relationship change under future warming is highly uncertain despite internal noises basically eliminated
- Both future changes in fraction of fast-decay ENSO and ENSO-WNPAC correlation of slow-decay ENSO determine the model spread
- Based on observational constraints, the trans-seasonal relationship will robustly strengthen under future high-emission scenarios

Supporting Information:

Supporting Information may be found in the online version of this article.

Correspondence to:

X. Chen,
chenxiaolong@mail.iap.ac.cn

Citation:

Wang, L., Chen, X., Zhao, Y., Zhou, T., Chen, L., & Sun, M. (2025). Enhanced trans-seasonal ENSO impact on East Asian-western Pacific climate in warmer future: An emergent constraint from multi-large ensembles. *Geophysical Research Letters*, *52*, e2025GL116648. https://doi.org/10.1029/2025GL116648

Received 22 APR 2025
Accepted 4 SEP 2025

Author Contributions:

Conceptualization: Lu Wang, Xiaolong Chen
Data curation: Xiaolong Chen, Yan Zhao
Formal analysis: Xiaolong Chen, Yan Zhao
Funding acquisition: Xiaolong Chen
Investigation: Xiaolong Chen, Yan Zhao
Methodology: Xiaolong Chen
Project administration: Lu Wang
Resources: Lu Wang
Software: Xiaolong Chen, Yan Zhao
Supervision: Lu Wang
Validation: Xiaolong Chen

Enhanced Trans-Seasonal ENSO Impact on East Asian-Western Pacific Climate in Warmer Future: An Emergent Constraint From Multi-Large Ensembles

Lu Wang[1], Xiaolong Chen[2], Yan Zhao[1], Tianjun Zhou[2,3], Lin Chen[1], and Ming Sun[1,4]

[1]State Key Laboratory of Climate System Prediction and Risk Management/Key Laboratory of Meteorological Disaster, Ministry of Education/Collaborative Innovation Center on Forecast and Evaluation of Meteorological Disasters, Nanjing University of Information Science and Technology, Nanjing, China, [2]State Key Laboratory of Earth System Numerical Modeling and Application, Institute of Atmospheric Physics, Chinese Academy of Sciences, Beijing, China, [3]University of Chinese Academy of Sciences, Beijing, China, [4]Anhui Climate Center, Anhui Meteorological Service, Hefei, China

Abstract Predicting the boreal summer climate over East Asia and the western Pacific is crucial for communities preparing for extreme events. A key source of predictability is the strong connection between the western North Pacific anomalous circulation (WNPAC) and the preceding El Niño-Southern Oscillation (ENSO). However, the potential change of this link under future greenhouse warming remains uncertain due to substantial internal variability and inter-model discrepancies. Here, by leveraging emergent constraints from multi-large ensemble simulations, we show that the trans-seasonal ENSO-WNPAC correlation robustly strengthens under high-emission scenarios, with a 67% reduction in the projection uncertainty. This enhancement indicates a 9% increase in the ENSO-contributed predictability (explained variance) of summer WNPAC. The spread across models primarily derives from their differing representations of ENSO-decaying regimes. Our results indicate a more predictable East Asian-western Pacific summer climate in a warmer world, offering encouraging prospects for adapting to anticipated increases in extremes associated with WNPAC.

Plain Language Summary The boreal summer climate over East Asia and the western Pacific are largely controlled by the western North Pacific anomalous cyclone/anticyclone (WNPAC). A key factor in the seasonal predictability of WNPAC is its strong connection to the El Niño-Southern Oscillation (ENSO) in the preceding winter. However, how human-caused global warming might change this cross-seasonal ENSO-WNPAC relationship is always controversial. By aggregating outputs from 8 state-of-the-art climate and Earth system models featuring large ensembles (totally 550 members) to eliminate influence of climate noises, we find that inter-model spread in future change of the ENSO-WNPAC relationship under high emission scenarios is rooted in the biases of the relationship related to different ENSO-decaying modes in the historical simulations. Most of the models underestimate the ENSO-WNPAC relationship in both the fast-decay and slow-decay ENSO events, that is weaker correlation than that in the present-day observation, and thus underestimate intensification of the relationship under future warming. Using our observationally based constraint, we project that the potential predictability of summer WNPAC contributed by the preceding ENSO (explained variance) will robustly increase by 9% with model spread reduced by 67%. The more predictable summer WNPAC is encouraging news for adapting to more frequent and intense future heatwaves, floods, and droughts brought by monsoon and tropical cyclones in East Asia and the western Pacific.

1. Introduction

The boreal summer western North Pacific anomalous circulation (WNPAC), manifesting as either an anomalous cyclone or anticyclone, significantly influences the climate across East Asia and the western Pacific (Chang et al., 2000; X. Chen & Zhou, 2018; T. Li et al., 2017; Wang et al., 2000, 2013; Zhang et al., 2017). It can modulate monsoon strength, shape precipitation patterns, influence the occurrence of extreme floods and droughts, and shift the tracks of tropical cyclones. Consequently, understanding how the predictability of the WNPAC might change under ongoing human-induced global climate change is crucial for improving future disaster prevention and climate risk management in these regions.

El Niño-Southern Oscillation (ENSO) is the leading predictor for the summer WNPAC (Harrison & Larkin, 1996; Kosaka et al., 2013; Stuecker et al., 2015; Wang et al., 2000; Xie et al., 2016). Typically, an El Niño (La Niña)

Visualization: Xiaolong Chen, Yan Zhao
Writing – original draft: Lu Wang, Xiaolong Chen
Writing – review & editing: Lu Wang, Xiaolong Chen, Tianjun Zhou, Lin Chen, Ming Sun

event in the preceding boreal winter is followed by an anticyclonic (cyclonic) WNPAC in the subsequent summer. This trans-seasonal linear relationship forms the basis for seasonal forecasting of the WNPAC, with stronger correlations indicating greater predictability. However, projecting future changes in the WNPAC-ENSO relationship is challenging. Internal variabilities within the climate system, such as the Interdecadal Pacific Oscillation (Song & Zhou, 2015), the Atlantic Multidecadal Oscillation (M. Xu et al., 2023), and fluctuations of sea surface temperature (SST) in Indian Ocean (L. Lin et al., 2025), act as inherent noise, modulating the strength and stability of the ENSO-WNPAC link. On the other hand, there are substantial discrepancies among climate models in their responses to external forcings, which further complicates the task to obtain reliable projections of future WNPAC predictability.

To address this, using Single Model Initial-condition Large Ensembles (SMILEs) from diverse models is ideal. SMILEs enable the separation of the forced response from internal variability and capture model spread in forced responses (Deser et al., 2020, 2024; Huang et al., 2020; M. Wu et al., 2021; Z. Zhou et al., 2024; S. Zhou et al., 2024). Despite this potential, no prior study has utilized multi-model SMILEs to examine future WNPAC responses to preceding ENSO. Previous studies have either relied on a single projection realization from multiple models or have been based on a single-model produced SMILE, yielding inconclusive results on this issue over the past decade (W. Chen et al., 2016; He et al., 2019; Hu et al., 2014; Jiang et al., 2018; S. Lin et al., 2024). For instance, the Coupled Model Intercomparison Project Phases 5 ensemble mean projects a weakened anomalous WNPAC, while the CMIP6 counterpart shows an opposite projection (He et al., 2022). The Community Earth System Model version 1 (CESM1) SMILE indicates minimal future changes in the ENSO-WNPAC relationship (M. Wu et al., 2021), while the Flexible Global Ocean-Atmosphere-Land System (FGOALS) SMILE suggests an intensification of this link (Ma et al., 2023). These conflicting results undermine the reliability of any conclusions drawn previously.

This study pioneers the use of multi-SMILEs to reexamine this issue. We propose a multi-step emergent constraint approach to reduce the projection uncertainty in the ENSO-WNPAC relationship across models by pinpointing its uncertainty source. Our refined projections indicate that under future high-emission scenarios, the interannual variance of WNPAC explained by ENSO will robustly increase by about 9%, with a reduction in model uncertainty by 67%. This enhancement in the correlation coefficient implies an improved seasonal predictability of the East Asian-western Pacific summer climate in the future.

2. Data and Methods

2.1. Model and Data

Eight SMILEs including historical simulation and future projection under high greenhouse-gas emission scenarios are used in this study (Table S1 in Supporting Information S1). To obtain robust forced signals of ENSO-related interannual variability change, we selected the SMILE which has larger than 40-initial-condition members (Z. Zhou et al., 2024). Projected changes during 2050–2099 relative to 1956–2005 are focused. Taking the advantage of SMILE approach, large-member mean of any variable can be regarded as its true "climatology" since impact of internal variability could be almost eliminated.

To assess model and constrain projection, data from ECMWF Reanalysis v5 (ERA5) during 1950–2024 (Soci et al., 2024) are also used. For showing patterns, all simulation and reanalysis data sets are interpolated onto a $2.5° \times 2.5°$ grid by bilinear method and detrended prior to analysis. More details of the used data are in Text S1 in Supporting Information S1.

2.2. Reconstruction of ENSO-WNPAC Correlation Coefficient

The ENSO-WNPAC relationship is defined by the correlation coefficient (hereafter $C_{E\text{-}W}$) between the Nino3.4 index in boreal winter (December–February, D(-1)JF) and the subsequent summer (June–August, JJA) WNPAC index (Text S2 in Supporting Information S1). The $C_{E\text{-}W}$ calculated using only ENSO years (C_{ENSO}) excellently approximates to that using all years (Figure S1a in Supporting Information S1). Thus, to clearly show the relative roles of different ENSO-decaying regimes (Text S2 in Supporting Information S1) on the uncertainty in projected $C_{E\text{-}W}$ change ($\Delta C_{E\text{-}W}$), under the assumption that fast-decay (F) and slow-decay (S) ENSO events are independent, we reconstruct the $\Delta C_{E\text{-}W}$ as follows:

$$\Delta C_{E-W} \approx \Delta C_{ENSO} \approx \Delta\left(f_F \times C_F + f_S \times C_S\right) \approx \Delta f_F \times C_{FH} + f_{FH} \times \Delta C_F + \Delta f_S \times C_{SH} + f_{SH} \times \Delta C_S, \quad (1)$$

in which f_F represents fraction of fast-decay ENSO relative to all the ENSO events, C_F the individual $C_{E\text{-}W}$ calculated using only fast-decay ENSO years, f_S and C_S for slow-decay ENSO, $f_F + f_S = 1$, and "H" in subscript for historical period. Nonlinear term is omitted in Equation 1. The accuracy of this reconstruction is verified in Figure S1b in Supporting Information S1.

2.3. Multi-Step Emergent Constraint

To constrain the projected ENSO-WNPAC relationship, we employ the emergent constraint method, which leverages the statistical relationship between observable variables in the historical period and projected changes of targeted variables across a multi-model ensemble (Bowman et al., 2018; X. Chen et al., 2020). Considering the distinct mechanisms of different ENSO-decaying regimes on WNPAC, a multi-step emergent constraint is proposed. More details are seen in Text S3 in Supporting Information S1.

3. Results

3.1. Uncertainty in ENSO-WNPAC Relationship Changes

The ERA5 reanalysis data reveal a significantly negative correlation between ENSO in the previous winter and summer 850-hPa vorticity over the western North Pacific, manifesting as an anticyclone stretching from the South China Sea to the subtropical North Pacific (Figure 1a). This WNPAC pattern is largely reproduced by the multi-model mean of historical simulations, expect for positive biases over the South China Sea and east of the Philippines (Figure 1b). However, when examining projected changes, the multi-model mean indicates an unclear evolution of the WNPAC pattern. This is evidenced by alternating positive and negative vorticity anomalies within the WNPAC region, as well as low inter-model consistency (Figure 1c).

To quantify the ENSO-WNPAC relationship and its projected changes across different models, we calculated the $C_{E\text{-}W}$ corresponding to each simulation, using the observed WNPAC region (the green box in Figure 1a) to define the WNPAC index, ensuring consistency and simplicity across the analysis. Most models significantly underestimate the observed mean $C_{E\text{-}W}$ (-0.39) during historical periods, except CESM2. The spread emulated from the resampled ERA5 data (gray line) is also close to that in the best model CESM2, although the resampling method may underestimate the impact of internal variability in observation.

Among the 8 models analyzed, two (CESM2 and FGOALS-g3) project a substantial strengthening of the ENSO-WNPAC relationship in the future, as indicated by a more negative $C_{E\text{-}W}$ (Figures 1h and 1i). Conversely, the remaining models show weakening or marginal changes, indicated by a more positive or unchanged $C_{E\text{-}W}$. The multi-model mean change in $C_{E\text{-}W}$ ($\Delta C_{E\text{-}W}$) is -0.04 ± 0.14 (± 1 inter-model standard deviation). Notably, the magnitude of this multi-model mean change (0.04) is smaller than both the observed internal variability (0.06) and the inter-model uncertainty (0.14). Consequently, the raw multi-model mean based on the 8 SMILEs does not provide a robust indication of how the trans-seasonal ENSO-WNPAC relationship will respond to future warming. The robustness of these findings is further confirmed by an additional analysis using model-specific region to define the ENSO-WNPAC relationship, which yields identical results (Text S4 and Figures S2–S4 in Supporting Information S1).

3.2. Mechanisms of ENSO-Decaying Regimes Impacting on ENSO-WNPAC Relationship

The ENSO-WNPAC relationship is governed by distinct physical processes during fast-decay versus slow-decay ENSO events.

In fast-decay ENSO years, the ENSO-WNPAC connection is primarily manifested as negative feedback of anomalous WNPAC on ENSO SST anomalies in the western-central Pacific (Figures 2a, 2c, and 2e). Taking the El Niño event for instance, the anomalous WNPAC during D(-1)JF is associated with cold SST anomalies and suppressed convections in the tropical western Pacific (Figure 2a), which are consequences of positive wind-evaporation-SST feedback and low moist enthalpy advection induced by the anomalous northeasterlies as a Gill-type response to the eastern-central Pacific heating (Wang et al., 2000; B. Wu et al., 2017). The anomalous easterlies south of the WNPAC can potentially suppress El Niño, propelling it toward its opposite phase. By

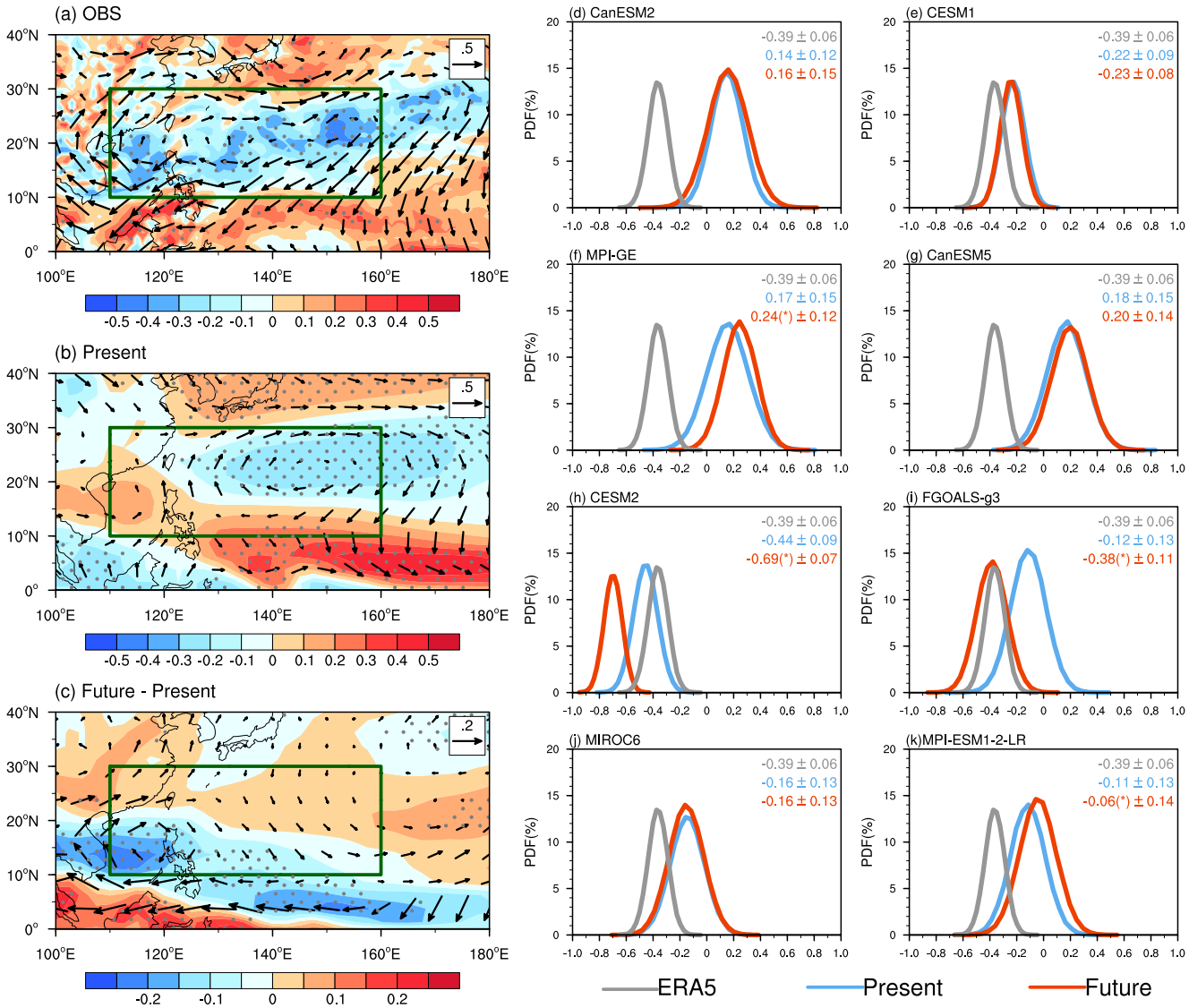

Figure 1. Correlation coefficient between El Niño-Southern Oscillation in the previous winter and low-level circulation in the following summer. (a) Patterns of the correlation coefficient between D(-1)JF Nino3.4 index and 850-hPa vorticity (shadings) and winds (vectors) in ERA5 (1950–2024), (b) multi-model mean in the historical period (1965–2005), and (c) changes in future (2050–2099) under RCP8.5/SSP5-8.5 scenario over the western North Pacific. Dotted shadings denote significance at the 5% level of *t*-test in panel (a) and more than 75% of models agreeing the same sign in panel (b, c). The green box is for defining the western North Pacific anomalous circulation (WNPAC) index. (d–k) Probability density functions of correlation coefficient ($C_{E\text{-}W}$) between D(-1)JF Nino3.4 and JJA WNPAC index for ERA5 (gray, 1950–2024) and each model's simulation in the present day (blue) and future (red), with mean and standard deviation labeled on the top-right corner. The standard deviations of historical and projection in each model are calculated across members while that of ERA5 is estimated by 50-yr resampling 50 times from the 75-yr data. $\Delta C_{E\text{-}W}$ significant at the 5% level of *t*-test is marked by an asterisk.

MAM, the anomalous easterlies over the tropical western Pacific become extraordinarily strong, coincident with a significantly weakened El Niño (Figure 2c). In JJA, these easterly anomalies are further intensified, extending to the central Pacific, transforming the Pacific condition into a La Niña, while the Indian Ocean basin-wide warming nearly vanishes (Figure 2e). The summer WNPAC is established through the intensified Walker circulation and local Hadley circulation between the Maritime Continent and western North Pacific (X. Chen & Zhou, 2014; Wang et al., 2013).

In contrast, during slow-decay ENSO years, the WNPAC's feedback on El Niño SST anomalies are considerably weak, possibly due to weaker Indian Ocean warming making anomalous equatorial easterlies unable to extend to 140°E (Figure 2b) compared with the fast-decay case (Figure 2a). The anomalous WNPAC is largely driven by El Niño-induced tropical Indo-Pacific anomalies throughout all the seasons (Figures 2b, 2d, and 2f).

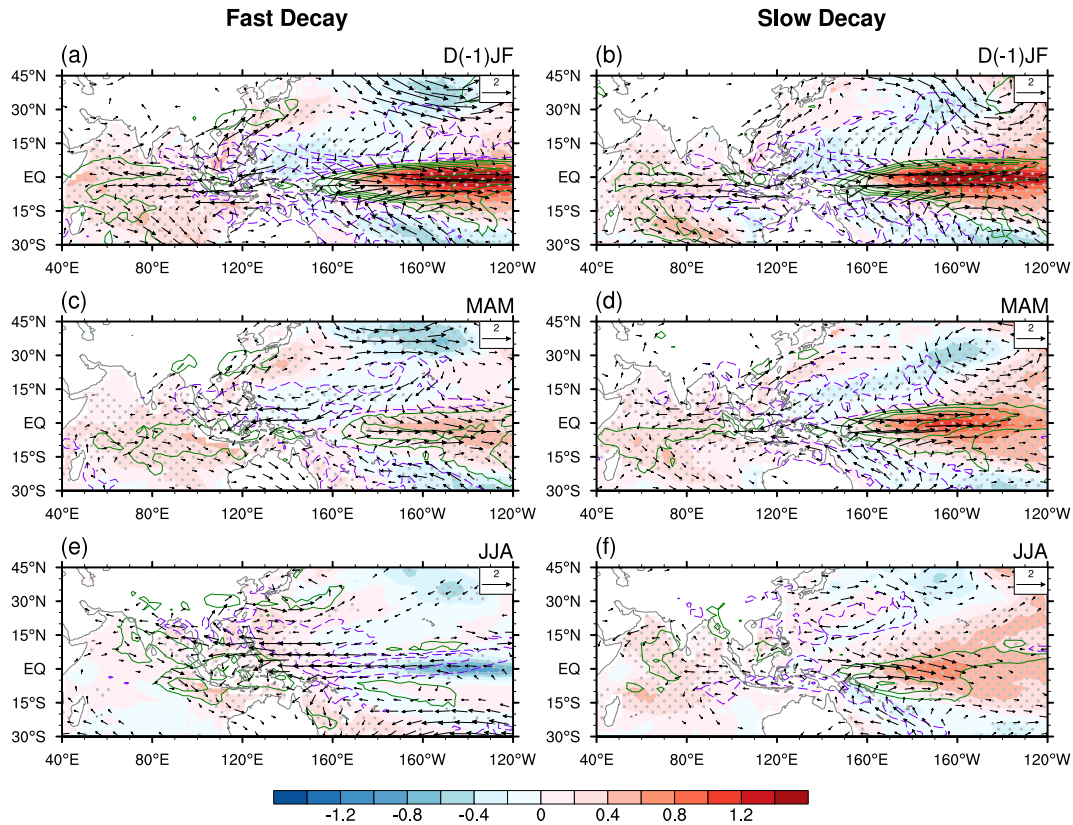

Figure 2. Observed seasonal evolutions of air-sea anomalies related to different El Niño-Southern Oscillation (ENSO)-decaying regimes. Regression coefficients of sea surface temperature (shadings, K), precipitation (contours from −3.5 to 3.5 by 1, mm day^{-1}), and 850-hPa wind (vectors, m s^{-1}) in (a, b) D(-1)JF, (c, d) MAM, and (e, f) JJA onto standardized D(-1)JF Nino3.4 index are shown for fast-decay (left) and slow-decay (right) ENSO years based on ERA5 during 1950–2024. Magnitude of anomalous wind larger than 0.3 m s^{-1} are drawn. Dotted shadings are significant at the 5% level of *t*-test.

For instance, from D(-1)JF to MAM, SST, precipitation, and circulation anomalies across the Indo-Pacific basin remain largely unchanged, except for a slight reduction in intensity (Figures 2b and 2d). The Indian Ocean basin warming, particularly in the Arabian Sea (X. Chen & Zhou, 2014), intensifies in JJA and sustains the anomalous WNPAC (Figure 2f) through eastward-propagating Kelvin waves and local Ekman divergence in the boundary layer (B. Wu et al., 2009; Xie et al., 2009), well-known as the "capacitor effect" of the Indian Ocean (Du et al., 2009; Yang et al., 2007).

Given the distinct physical processes that influence the ENSO-WNPAC relationship in fast-decay versus slow-decay ENSO events, we decompose the uncertainty in $\Delta C_{E\text{-}W}$ according to these two ENSO-decaying regimes. Specifically, $\Delta C_{E\text{-}W}$ is linearly decomposed into contributions from changes in the *fraction* of events (Δf_F and Δf_S) and changes in the *individual correlation* for each regime (ΔC_F and ΔC_S), as detailed in Section 2.2. This decomposition perfectly reconstructs the original $\Delta C_{E\text{-}W}$ for each model and explains the inter-model spread very well (Figure S1b in Supporting Information S1).

Based on this decomposition, we find that the inter-model uncertainty in $\Delta C_{E\text{-}W}$ is predominantly driven by two factors: Δf_F and ΔC_S. Together, Δf_F and ΔC_S account for 88% of the inter-model variance of $\Delta C_{E\text{-}W}$ (Figure S1e in Supporting Information S1), with both factors making comparable contributions (Figures 3a and 3b). In contrast, the uncertainties associated with ΔC_F and Δf_S are negligible (Figures S1c and S1d in Supporting Information S1). This indicates that Equation 1 can be further simplified to ($\Delta f_F \times C_{FH} + f_{SH} \times \Delta C_S$). Therefore, accurately constraining Δf_F and ΔC_S with present-day observations offers a viable pathway to correct the models' projections of $\Delta C_{E\text{-}W}$ and substantially reduce its uncertainty.

To establish an emergent constraint relationship for Δf_F, we consider the seasonal air-sea interaction related to fast-decay ENSO events, which features a strong coupling between WNPAC and ENSO prompting a swift

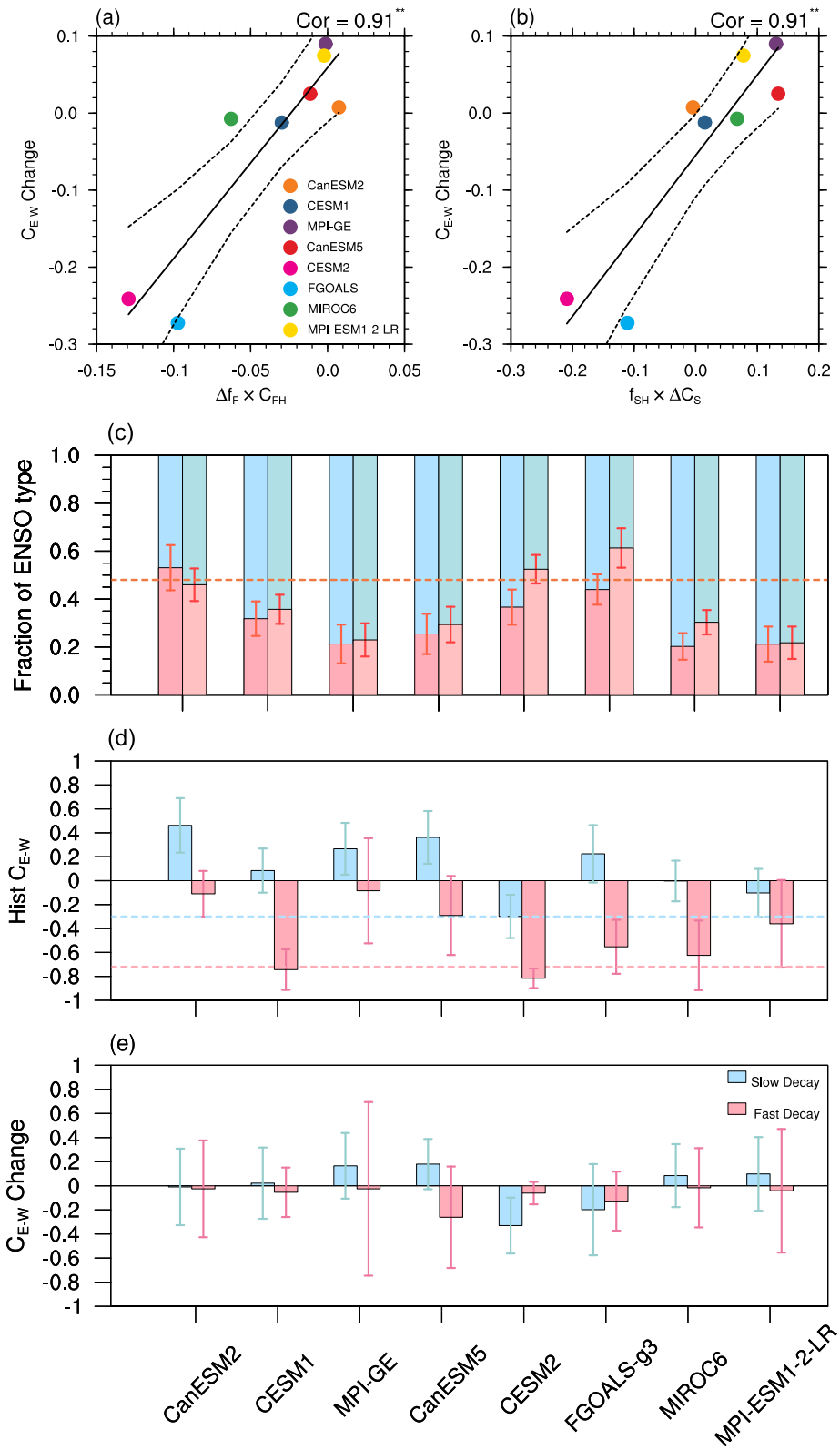

Figure 3.

transition of ENSO to its opposite phase (Figures 2a, 2c, and 2e). As global warming is expected to amplify the impact of El Niño on tropical circulations and convections through increased moisture and clouds (Hu et al., 2021; Sun et al., 2020), we hypothesize that a stronger ENSO-WNPAC coupling (represented by C_F) in the present day would favor a greater increase in the fraction of fast-decay events (Δf_F) in a warmer future. This hypothesis is strongly supported by the models: CESM1, CESM2, FGOALS-g3, and MIROC6, which simulate a historically strong negative C_F (closely matching ERA5 reanalysis; Figure 3d), also project a substantial increase in Δf_F (Figure 3c). The robust inter-model correlation coefficient (-0.73, $p < 0.05$) between historical C_F and future Δf_F confirms the efficacy of this emergent constraint.

In contrast, the JJA WNPAC anomaly during slow-decay ENSO events is primarily driven by persistent influence of tropical anomalies from D(-1)JF (Figure 2b), particularly through the Indian Ocean capacitor effect (Figure 2f). Models that simulate a stronger historical ENSO intensity (σ_S) tend to maintain its strength as well as the trans-seasonal impacts under future warming (Figures S5a–S5c in Supporting Information S1). Consequently, they project a more pronounced El Niño-induced warming in the Arabian Sea in JJA (Figure S5c in Supporting Information S1), consistent with observations (Figure 2f). This enhanced Arabian Sea warming is expected to further amplify both local convections and the remote suppressions over the WNP during the ENSO-decaying phase, via a strengthened capacitor effect (Figure S5d in Supporting Information S1). Therefore, the historical intensity of slow-decay ENSO events (σ_S) serves as a key predictor for the future change in the corresponding correlation (ΔC_S), as the underlying thermodynamic response to ENSO is amplified under warming, even if ENSO intensity itself remains constant (Sun et al., 2020). Our analysis reveals a strong, significant inter-model correlation (-0.82, $p < 0.05$) between historical σ_S and projected ΔC_S, establishing a physically based emergent constraint for this component.

3.3. Multi-Step Emergent Constraints Based on ENSO-Decaying Regimes

Utilizing the above constraints for Δf_F and ΔC_S, we implement a multi-step emergent constraint methodology, as illustrated in the flowchart (Figure 4), beginning by individually constraining Δf_F and ΔC_S (Figures 4a–4c). Subsequently, the constrained Δf_F and ΔC_S, along with the observed C_{FH} and f_{SH} are used to constrain the total $\Delta C_{E\text{-}W}$ (Figure 4d). The observed probability density functions of C_{FH} and f_{SH} (-0.72 ± 0.085 and 0.52 ± 0.051, respectively) are also derived from ERA5 data through the resampling method (Text S3 in Supporting Information S1).

Most of the models overestimate the slow-decay ENSO intensity (σ_S) but meanwhile underestimate the C_S (Figure 3d), implying that for models the σ_S would need to be stronger if the simulated C_S could be consistent with the observation. To address this, we first project the observed C_S onto model space to derive a best-estimated σ_S, leveraging the inter-model relationship between C_S and σ_S in the historical period that stronger C_S corresponds to larger σ_S (Figure 4a). This estimated σ_S, deemed the optimal value in model space, is then employed to constrain ΔC_S (Figure 4b).

Since most of the models underestimate both the C_S and C_F in the historical period (Figures 4a and 4c), after implementing the emergent constraints, Δf_F exhibits a significant increase ($11\% \pm 6\%$ vs. raw $6\% \pm 8\%$, Figure 4c), and ΔC_S is enhanced as well (-0.07 ± 0.14 vs. raw 0.00 ± 0.18, Figure 4b). As the illustrated mechanisms underlying the constraint relationships above, both of the constrained Δf_F and ΔC_S can be expected from amplified influence of El Niño under warming. Consequently, the constrained $\Delta C_{E\text{-}W}$, at -0.10 ± 0.08 (Figure 4d), robustly indicates a strengthening of the ENSO-WNPAC relationship under future warming conditions, contrasting with the raw projection of -0.04 ± 0.14 from the multi-model mean of SMILEs. It means that

Figure 3. Model uncertainty of El Niño-Southern Oscillation (ENSO)-western North Pacific anomalous circulation relationship changes related to different ENSO-decaying regimes. (a) Contribution of fast-decay ENSO fraction change to total $\Delta C_{E\text{-}W}$ across models. (b) Same as (a) but for the contribution of $\Delta C_{E\text{-}W}$ of slow-decay ENSO. Solid black lines in panels (a, b) are linear fitting across models and dashed lines show 95% ranges of the estimated mean $\Delta C_{E\text{-}W}$ based on the linear fitting. Values on the top-right corner in panels (a, b) are correlation coefficients across models, with two asterisks indicating the statistical significance exceeding the 5% level under *t*-test. (c) The fractions of fast-decay (red) and slow-decay (blue) ENSO events relative to total ENSO events during historical (left column) and future (right column) periods in each model, respectively. The dashed red line denotes the observed faction of fast-decay ENSO in ERA5 during 1950–2024. (d) Multi-member mean of $C_{E\text{-}W}$ for each model in fast-decay (red) and slow-decay (blue) ENSO events in the historical period (1956–2005). Red and blue dashed lines denote the observed $C_{E\text{-}W}$ in fast-decay and slow-decay ENSO events, respectively, based on the 75-yr ERA5 data. (e) Same as (d) but for future changes (2050–2099) relative to the historical period. Bars in panels (c–e) denote $\pm 1\sigma$ across members.

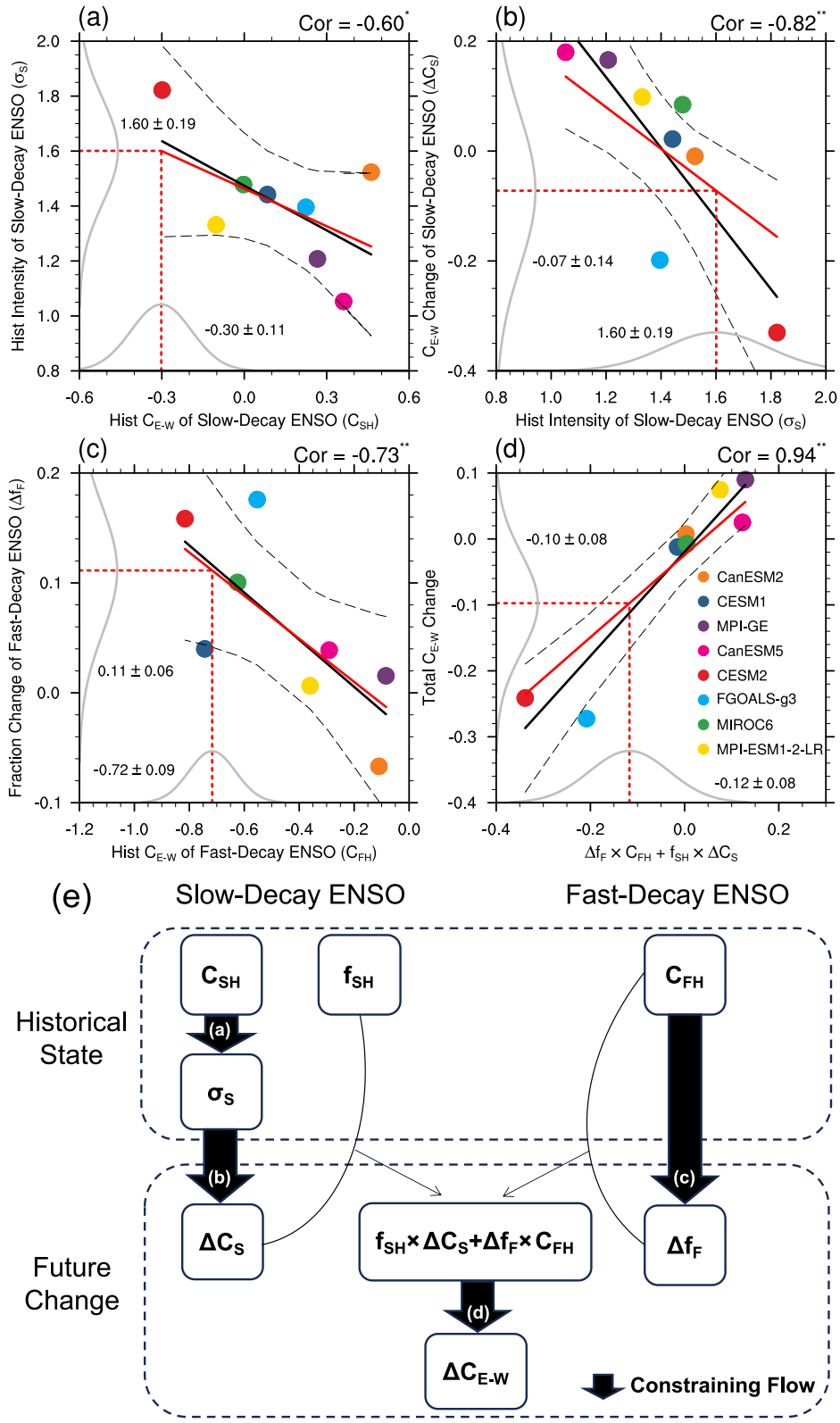

Figure 4.

the variance of summer WNPAC on a 50-year scale explained by ENSO in the previous winter will rise by about 9%, meanwhile the projection uncertainty reduced by 67%.

4. Conclusions

Projecting future responses of internal variability to external forcing is an important but rather challenging task, due to very low signal-to-noise ratio from both the intrinsic randomness of complex coupled system and the inter-model response uncertainty to external forcings. Focusing on how the trans-seasonal ENSO-WNPAC relationship will change in warmer future, we develop multi-step emergent constraints based on multi-SMILEs to address the projection uncertainties in this well-known source of predictability of East Asia-western Pacific summer climate. Main conclusions are summarized as follows.

The raw projections show a non-significant future change of ENSO-WNPAC relationship, that is correlation coefficient between D(-1)JF Nino3.4 index and JJA WNPAC index ($\Delta C_{E\text{-}W} = -0.04 \pm 0.14$), primarily due to existence of large inter-model uncertainty even after most internal noises eliminated by averaging large members in each model. By linearly decomposing the $\Delta C_{E\text{-}W}$ according to different ENSO-decaying regimes, we identify that the model uncertainty in $\Delta C_{E\text{-}W}$ is mainly contributed by changes in the fraction of fast-decay ENSO events (Δf_F) and changes in the correlation coefficient for slow-decay ENSO events (ΔC_S). These two factors can explain 88% of the inter-model variance. Further, we find that the model response uncertainty in Δf_F and ΔC_S can be eventually traced back to the ENSO-WNPAC correlations in historical simulation under fast and slow ENSO-decaying regimes, that is C_F and C_S, respectively. The constrained result indicates that the ENSO-explained variance of WNPAC will increase by about 9% ($C_{E\text{-}W}$ enhancing from -0.39 to -0.49), along with model uncertainty reduced by 67% (inter-model variance decreasing from 0.14^2 to 0.08^2). The multi-step emergent constraints are well established on the mechanisms of trans-seasonal interactions between ENSO and WNPAC under different ENSO-decaying regimes.

5. Discussion

It is noted that most models are strongly biased in simulating the historical $C_{E\text{-}W}$ compared with ERA5 (Figures 1d–1k). One may argue that such a large bias could disqualify these models to be used in future projection. Selecting "good" model to project future change is a natural thought in conventional model assessment framework. However, in emergent constraint framework, model bias is not a negative label but useful information. As long as model numbers are large enough in a multi-model ensemble, larger biases in some models serve to establish more clear and robust constraining relationship between historical biases and future projection across models. Through understanding how different model biases in historical period lead to diverse projections, model biases provide important insight to constrain future changes.

Due to data availability of multi-model large ensembles, the emergent constraint in this study is only implemented for high-emission scenarios (RCP8.5/SSP5-8.5). To examine if it is still valid under lower emission scenario, three CMIP6 models providing large-ensemble simulations under the SSP2-4.5, that is CanESM5 (50 members), MIROC6 (50 members), and MPI-ESM1-2-LR (30 members), are used to compare the projected $C_{E\text{-}W}$ with that under SSP5-8.5 (Figure S6 in Supporting Information S1). The result shows that the projected $C_{E\text{-}W}$ under SSP2-4.5 and SSP5-8.5 is close to each other in each model. The slight differences are well within the range of internal variability, statistically non-significant. Therefore, the emergent constraint and consequential results should be also valid for lower emission scenarios, at least the SSP2-4.5.

Figure 4. Multi-step emergent constraints on El Niño-Southern Oscillation (ENSO)-western North Pacific anomalous circulation relationship changes based on different ENSO-decaying regimes. (a, b) The first two steps are for constraining $C_{E\text{-}W}$ change of slow-decay ENSO (ΔC_S) based on observed $C_{E\text{-}W}$ of slow-decay ENSO in historical period (C_{SH}), (c) the third step for constraining fraction change of fast-decay ENSO (Δf_F) based on observed $C_{E\text{-}W}$ of fast-decay ENSO in historical period (C_{FH}), and (d) the last step for constraining the total $\Delta C_{E\text{-}W}$ based on the constrained ΔC_S and Δf_F in panels (b, c), multiplying observed f_{SH} and C_{FH} in historical period, respectively. Solid black lines are linear fitting across models and long-dashed black lines show 95% ranges of the estimated mean change of variables on the *Y*-axis based on the linear fitting. Values on the top-right corner are correlation coefficients across models, with one asterisk (two asterisks) indicating the statistical significance at the 10% (5%) level under *t*-test. Red solid lines are adjusted slopes of the constraint relationship in the hierarchical statistical framework according to Equation 2 in Text S3 in Supporting Information S1. Red short-dashed lines show constrained expectations, with corresponding probability density functions (PDFs) under Gaussian assumption attached along the *X* and *Y* axes. The PDFs in panels (a, c, and d) on the *X*-axis are estimated through 50-yr resampling 50 times from the 75-yr ERA5 data. (e) Flowchart summarizing the multi-step emergent constraints in panels (a–d).

Potential changes in the predictability of the surface temperature and precipitation in future have been extensively investigated (Boer, 2009; Le et al., 2023; S. Li et al., 2020; Mamalakis et al., 2018; Wang et al., 2015; L. Xu et al., 2020), whereas the circulation predictability is rarely involved. Without assuming how ENSO predictability would change, our study indicates a more predictable WNPAC with a lead time of two seasons. Considering extreme El Niño and La Niña would occur more frequently under greenhouse warming (Cai et al., 2014, 2015), predicting extremes related to the WNPAC in boreal summer would be hopefully further improved in future. The possibly intensified predictability of WNPAC deserves to be verified by nudging mean state of SST or atmospheric moisture to the projected states in a seasonal prediction system. Because the western Pacific, including East Asia and Southeast Asia, long suffers from disasters of the abnormal monsoon, super typhoons, heatwaves, floods, and droughts, the potential increase in predictability of the western Pacific climate in a warmer future could facilitate climate adaptations for this densely populated area.

Conflict of Interest

The authors declare no conflicts of interest relevant to this study.

Data Availability Statement

The ERA5 reanalysis is provided by ECMWF on Copernicus Climate Change Service (C3S) Climate Data Store (CDS) (Hersbach et al., 2023a, 2023b). The availability of the model simulation data from 8 SMILEs are described below: CanESM2 are available at Environment and Climate Change Canada (https://crd-data-donnees-rdc.ec.gc.ca/CCCMA/products/CanSISE/output/CCCma/CanESM2/), CESM1 and CESM2 at UCAR/NCAR Climate Data Gateway (Danabasoglu et al., 2020; Kay et al., 2021), MPI-GE on a data port provided by DKRZ (https://esgf-metagrid.cloud.dkrz.de/search), FGOALS-g3 at Science Data Bank (Zhao et al., 2023), CanESM5, MIROC6, MPI-ESM1-2-LR at the Earth System of Grid Federation (https://esgf-node.ornl.gov/search).

Acknowledgments
This study is supported by the National Key Research and Development Program of China (Grant 2020YFA0608904) and Excellent Youth Natural Science Foundation of Jiangsu Province (BK20230061). We acknowledge the High Performance Computing Center of Nanjing University of Information Science & Technology for their support of this work.

References

Boer, G. J. (2009). Changes in interannual variability and decadal potential predictability under global warming. *Journal of Climate*, *22*(11), 3098–3109. https://doi.org/10.1175/2008JCLI2835.1

Bowman, K. W., Cressie, N., Qu, X., & Hall, A. (2018). A hierarchical statistical framework for emergent constraints: Application to snow-albedo feedback. *Geophysical Research Letters*, *45*(23), 13050–13059. https://doi.org/10.1029/2018GL080082

Cai, W., Wang, G., Santoso, A., McPhaden, M. J., Collins, M., Vecchi, G., et al. (2014). Increasing frequency of extreme El Niño events due to greenhouse warming. *Nature Climate Change*, *4*, 111–116. https://doi.org/10.1038/nclimate2100

Cai, W., Wang, G., Santoso, A., McPhaden, M. J., Wu, L., Jin, F.-F., et al. (2015). Increased frequency of extreme La Niña events under greenhouse warming. *Nature Climate Change*, *5*(2), 132–137. https://doi.org/10.1038/nclimate2492

Chang, C.-P., Zhang, Y., & Li, T. (2000). Interannual and interdecadal variations of the East Asian summer monsoon and tropical Pacific SSTs. Part I: Roles of the subtropical ridge. *Journal of Climate*, *13*(24), 4310–4325. https://doi.org/10.1175/1520-0442(2000)013<4310:IAIVOT>2.0.CO;2

Chen, W., Lee, J.-Y., Ha, K.-J., Yun, K.-S., & Lu, R. (2016). Intensification of the western North Pacific anticyclone response to the short decaying El Niño event due to greenhouse warming. *Journal of Climate*, *29*(10), 3607–3627. https://doi.org/10.1175/JCLI-D-15-0195.1

Chen, X., & Zhou, T. (2014). Relative role of tropical SST forcing in the 1990s periodicity change of the Pacific-Japan pattern interannual variability. *Journal of Geophysical Research: Atmospheres*, *119*(23), 13043–13066. https://doi.org/10.1002/2014JD022064

Chen, X., & Zhou, T. (2018). Relative contributions of external SST forcing and internal atmospheric variability to July–August heat waves over the Yangtze River valley. *Climate Dynamics*, *51*(11–12), 4403–4419. https://doi.org/10.1007/s00382-017-3871-y

Chen, X., Zhou, T., Wu, P., Guo, Z., & Wang, M. (2020). Emergent constraints on future projections of the western North Pacific subtropical high. *Nature Communications*, *11*(1), 2802. https://doi.org/10.1038/s41467-020-16631-9

Danabasoglu, G., Deser, C., Rodgers, K., & Timmermann, A. (2020). CESM2 large ensemble [Dataset]. *Research Data Archive at the National Center for Atmospheric Research, Computational and Information Systems Laboratory*. https://doi.org/10.26024/kgmp-c556

Deser, C., Lehner, F., Rodgers, K. B., Ault, T., Delworth, T. L., DiNezio, P. N., et al. (2020). Insights from Earth system model initial-condition large ensembles and future prospects. *Nature Climate Change*, *10*(4), 277–286. https://doi.org/10.1038/s41558-020-0731-2

Deser, C., Phillips, A. S., Alexander, M. A., Amaya, D. J., Capotondi, A., Jacox, M. G., & Scott, J. D. (2024). Future changes in the intensity and duration of marine heat and cold waves: Insights from coupled model initial-condition large ensembles. *Journal of Climate*, *37*(6), 1877–1902. https://doi.org/10.1175/JCLI-D-23-0278.1

Du, Y., Xie, S.-P., Huang, G., & Hu, K. (2009). Role of air–sea interaction in the long persistence of El Niño–induced North Indian Ocean warming. *Journal of Climate*, *22*(8), 2023–2038. https://doi.org/10.1175/2008JCLI2590.1

Harrison, D. E., & Larkin, N. K. (1996). The COADS sea level pressure signal: A near-global El Nino composite and time series view, 1946-1993. *Journal of Climate*, *9*(12), 3025–3055. https://doi.org/10.1175/1520-0442(1996)009<3025:TCSLPS>2.0.CO;2

He, C., Cui, Z., & Wang, C. (2022). Response of western North Pacific anomalous anticyclones in the summer of decaying El Niño to global warming: Diverse projections based on CMIP6 and CMIP5 models. *Journal of Climate*, *35*, 359–372. https://doi.org/10.1175/JCLI-D-21-0352.1

He, C., Zhou, T., & Li, T. (2019). Weakened anomalous western North Pacific anticyclone during an El Niño–decaying summer under a warmer climate: Dominant role of the weakened impact of the tropical Indian Ocean on the atmosphere. *Journal of Climate*, *32*(1), 213–230. https://doi.org/10.1175/JCLI-D-18-0033.1

Hersbach, H., Bell, B., Berrisford, P., Biavati, G., Horányi, A., Muñoz Sabater, J., et al. (2023a). ERA5 monthly averaged data on pressure levels from 1940 to present [Dataset]. *Copernicus Climate Change Service (C3S) Climate Data Store (CDS)*. https://doi.org/10.24381/cds.6860a573

Hersbach, H., Bell, B., Berrisford, P., Biavati, G., Horányi, A., Muñoz Sabater, J., et al. (2023b). ERA5 monthly averaged data on single levels from 1940 to present [Dataset]. *Copernicus Climate Change Service (C3S) Climate Data Store (CDS)*. https://doi.org/10.24381/cds.f17050d7

Hu, K., Huang, G., Huang, P., Kosaka, Y., & Xie, S.-P. (2021). Intensification of El Niño-induced atmospheric anomalies under greenhouse warming. *Nature Geoscience*, *14*(6), 377–382. https://doi.org/10.1038/s41561-021-00730-3

Hu, K., Huang, G., Zheng, X.-T., Xie, S.-P., Qu, X., Du, Y., & Liu, L. (2014). Interdecadal variations in ENSO influences on Northwest Pacific–East Asian early summertime climate simulated in CMIP5 models. *Journal of Climate*, *27*(15), 5982–5998. https://doi.org/10.1175/JCLI-D-13-00268.1

Huang, X., Zhou, T., Dai, A., Li, H., Li, C., Chen, X., et al. (2020). South Asian summer monsoon projections constrained by the interdecadal Pacific oscillation. *Science Advances*, *6*(11), eaay6546. https://doi.org/10.1126/sciadv.aay6546

Jiang, W., Huang, G., Huang, P., & Hu, K. (2018). Weakening of Northwest Pacific anticyclone anomalies during post–El Niño summers under global warming. *Journal of Climate*, *31*(9), 3539–3555. https://doi.org/10.1175/JCLI-D-17-0613.1

Kay, J. E., Deser, C., Phillips, A. S., & Simpson, I. R. (2021). CESM1 large ensemble community project [Dataset]. *Research Data Archive at the National Center for Atmospheric Research, Computational and Information Systems Laboratory*. https://doi.org/10.5065/D6J101D1

Kosaka, Y., Xie, S., Lau, N., & Vecchi, G. A. (2013). Origin of seasonal predictability for summer climate over the northwestern Pacific. *Proceedings of the National Academy of Sciences of the United States of America*, *110*(19), 7574–7579. https://doi.org/10.1073/pnas.1215582110

Le, P. V. V., Randerson, J. T., Willett, R., Wright, S., Smyth, P., Guilloteau, C., et al. (2023). Climate-driven changes in the predictability of seasonal precipitation. *Nature Communications*, *14*(1), 3822. https://doi.org/10.1038/s41467-023-39463-9

Li, S., Wu, L., Yang, Y., Geng, T., Cai, W., Gan, B., et al. (2020). The Pacific Decadal Oscillation less predictable under greenhouse warming. *Nature Climate Change*, *10*(1), 30–34. https://doi.org/10.1038/s41558-019-0663-x

Li, T., Wang, B., Wu, B., Zhou, T., Chang, C.-P., & Zhang, R. (2017). Theories on formation of an anomalous anticyclone in western North Pacific during El Niño: A review. *Journal of Meteorological Research*, *31*(6), 987–1006. https://doi.org/10.1007/s13351-017-7147-6

Lin, L., Hu, C., Zhang, C., & Chen, D. (2025). Gradually disappearing cross-seasonal teleconnection between ENSO and Tibetan Plateau upper-level westerlies. *Geophysical Research Letters*, *52*(5), e2025GL115002. https://doi.org/10.1029/2025GL115002

Lin, S., Dong, B., & Yang, S. (2024). Enhanced impacts of ENSO on the Southeast Asian summer monsoon under global warming and associated mechanisms. *Geophysical Research Letters*, *51*(2), e2023GL106437. https://doi.org/10.1029/2023GL106437

Ma, J., Lin, P., Wang, L., Zhao, B., & Xu, H. (2023). Increasing connections of the leading internal mode of the summertime Northwest Pacific subtropical anticyclone with preceding ENSO under greenhouse warming in FGOALS-g3 super-large ensemble. *International Journal of Climatology*, *43*(13), 6164–6178. https://doi.org/10.1002/joc.8197

Mamalakis, A., Yu, J.-Y., Randerson, J. T., AghaKouchak, A., & Foufoula-Georgiou, E. (2018). A new interhemispheric teleconnection increases predictability of winter precipitation in Southwestern US. *Nature Communications*, *9*(1), 2332. https://doi.org/10.1038/s41467-018-04722-7

Soci, C., Hersbach, H., Simmons, A., Poli, P., Bell, B., Berrisford, P., et al. (2024). The ERA5 global reanalysis from 1940 to 2022. *Quarterly Journal of the Royal Meteorological Society*, *150*(764), 4014–4048. https://doi.org/10.1002/qj.4803

Song, F., & Zhou, T. (2015). The crucial role of internal variability in modulating the decadal variation of the East Asian summer monsoon–ENSO relationship during the twentieth century. *Journal of Climate*, *28*(18), 7093–7107. https://doi.org/10.1175/JCLI-D-14-00783.1

Stuecker, M. F., Jin, F.-F., Timmermann, A., & McGregor, S. (2015). Combination mode dynamics of the anomalous northwest Pacific anticyclone. *Journal of Climate*, *28*(3), 1093–1111. https://doi.org/10.1175/JCLI-D-14-00225.1

Sun, N., Zhou, T., Chen, X., Endo, H., Kitoh, A., & Wu, B. (2020). Amplified tropical Pacific rainfall variability related to background SST warming. *Climate Dynamics*, *54*(3–4), 2387–2402. https://doi.org/10.1007/s00382-020-05119-3

Wang, B., Wu, R., & Fu, X. (2000). Pacific–East Asian teleconnection: How does ENSO affect East Asian climate? *Journal of Climate*, *13*(9), 1517–1536. https://doi.org/10.1175/1520-0442(2000)013<1517:PEATHD>2.0.CO;2

Wang, B., Xiang, B., & Lee, J.-Y. (2013). Subtropical high predictability establishes a promising way for monsoon and tropical storm predictions. *Proceedings of the National Academy of Sciences of the United States of America*, *110*(8), 2718–2722. https://doi.org/10.1073/pnas.1214626110

Wang, B., Xiang, B., Li, J., Webster, P. J., Rajeevan, M. N., Liu, J., & Ha, K.-J. (2015). Rethinking Indian monsoon rainfall prediction in the context of recent global warming. *Nature Communications*, *6*(1), 7154. https://doi.org/10.1038/ncomms8154

Wu, B., Zhou, T., & Li, T. (2009). Seasonally evolving dominant interannual variability modes of East Asian climate. *Journal of Climate*, *22*(11), 2992–3005. https://doi.org/10.1175/2008JCLI2710.1

Wu, B., Zhou, T., & Li, T. (2017). Atmospheric dynamic and thermodynamic processes driving the western North Pacific anomalous anticyclone during El Niño. Part I: Maintenance mechanisms. *Journal of Climate*, *30*(23), 9621–9635. https://doi.org/10.1175/JCLI-D-16-0489.1

Wu, M., Zhou, T., & Chen, X. (2021). The source of uncertainty in projecting the anomalous western North Pacific anticyclone during El Niño–decaying summers. *Journal of Climate*, *34*, 6603–6617. https://doi.org/10.1175/JCLI-D-20-0904.1

Xie, S.-P., Hu, K., Hafner, J., Tokinaga, H., Du, Y., Huang, G., & Sampe, T. (2009). Indian Ocean capacitor effect on Indo-Western Pacific climate during the summer following El Niño. *Journal of Climate*, *22*(3), 730–747. https://doi.org/10.1175/2008JCLI2544.1

Xie, S.-P., Kosaka, Y., Du, Y., Hu, K., Chowdary, J. S., & Huang, G. (2016). Indo-Western Pacific Ocean capacitor and coherent climate anomalies in post-ENSO summer: A review. *Advances in Atmospheric Sciences*, *33*(4), 411–432. https://doi.org/10.1007/s00376-015-5192-6

Xu, L., Zhang, C., Chen, N., Moradkhani, H., Chu, P.-S., & Zhang, X. (2020). Potential precipitation predictability decreases under future warming. *Geophysical Research Letters*, *47*(22), e2020GL090798. https://doi.org/10.1029/2020GL090798

Xu, M., Xu, H., Ma, J., & Deng, J. (2023). Modulation of Atlantic Multidecadal Oscillation on ENSO-East Asian early summer monsoon connection: Role of a tropical pathway. *Climate Dynamics*, *61*(9–10), 4301–4318. https://doi.org/10.1007/s00382-023-06811-w

Yang, J., Liu, Q., Xie, S.-P., Liu, Z., & Wu, L. (2007). Impact of the Indian Ocean SST basin mode on the Asian summer monsoon. *Geophysical Research Letters*, *34*(2), L02708. https://doi.org/10.1029/2006GL028571

Zhang, R., Min, Q., & Su, J. (2017). Impact of El Niño on atmospheric circulations over East Asia and rainfall in China: Role of the anomalous western North Pacific anticyclone. *Science China Earth Sciences*, *60*(6), 1124–1132. https://doi.org/10.1007/s11430-016-9026-x

Zhao, B., Lin, P., Wei, J., Chen, X., & Liu, H. (2023). FGOALS-g3 super-large ensemble simulation [Dataset]. *Science Data Bank*. https://doi.org/10.11922/sciencedb.01332

Zhou, S., Huang, P., Wang, L., Hu, K., Huang, G., & Hu, P. (2024). Robust changes in global subtropical circulation under greenhouse warming. *Nature Communications*, *15*(1), 96. https://doi.org/10.1038/s41467-023-44244-5

Zhou, Z., Chen, X., Zhou, T., & Wu, B. (2024). Relationship between South Asian summer monsoon and ENSO primarily modulated by ENSO intensity based on two super large ensembles. *Climate Dynamics*, *62*, 10265–10279. https://doi.org/10.1007/s00382-024-07450-5

References From the Supporting Information

Eyring, V., Bony, S., Meehl, G. A., Senior, C. A., Stevens, B., Stouffer, R. J., & Taylor, K. E. (2016). Overview of the Coupled Model Intercomparison Project Phase 6 (CMIP6) experimental design and organization. *Geoscientific Model Development*, *9*(5), 1937–1958. https://doi.org/10.5194/gmd-9-1937-2016

Hu, S., Wang, L., Chen, X., Zhou, T., & Hsu, P.-C. (2024). Emergent constraints on future projections of Tibetan Plateau warming in winter. *Geophysical Research Letters*, *51*(9), e2024GL108728. https://doi.org/10.1029/2024GL108728

Kim, M., & Lee, E. (2022). Validation and comparison of climate reanalysis data in the East Asian monsoon region. *Atmosphere*, *13*(10), 1589. https://doi.org/10.3390/atmos13101589

Lin, P., Zhao, B., Wei, J., Liu, H., Zhang, W., Chen, X., et al. (2022). The Super-large ensemble experiments of CAS FGOALS-g3. *Advances in Atmospheric Sciences*, *39*(10), 1746–1765. https://doi.org/10.1007/s00376-022-1439-1

Maher, N., Milinski, S., Suarez-Gutierrez, L., Botzet, M., Dobrynin, M., Kornblueh, L., et al. (2019). The Max Planck Institute Grand Ensemble: Enabling the exploration of climate system variability. *Journal of Advances in Modeling Earth Systems*, *11*, 1–21. https://doi.org/10.1029/2019MS001639

O'Neil, B. C., Tebaldi, C., van Vuuren, D. P., Eyring, V., Friedlingstein, P., Hurtt, G., et al. (2016). The scenario model intercomparison project (ScenarioMIP) for CMIP6. *Geoscientific Model Development*, *9*, 3461–3482. https://doi.org/10.5194/gmd-9-3461-2016

Rodgers, K. B., Lee, S.-S., Rosenbloom, N., Timmermann, A., Danabasoglu, G., Deser, C., et al. (2021). Ubiquity of human-induced changes in climate variability. *Earth System Dynamics*, *12*(4), 1393–1411. https://doi.org/10.5194/esd-12-1393-2021

Taylor, K. E., Stouffer, R. J., & Meehl, G. A. (2012). An overview of CMIP5 and the experiment design. *Bulletin of the American Meteorological Society*, *93*(4), 485–498. https://doi.org/10.1175/BAMS-D-11-00094.1

Wu, M., Zhou, T., Chen, X., & Wu, B. (2020). Intermodel uncertainty in the projection of the Anomalous western North Pacific anticyclone associated with El Niño under global warming. *Geophysical Research Letters*, *47*(2), e2019GL086139. https://doi.org/10.1029/2019GL086139